THE ASTRONOMICAL JOURNAL VOLUME 110, NUMBER 2 AUGUST 1995

AN *IRAS*-SELECTED SEYFERT 2 GALAXY IRAS 18325−5926: THE X-RAY SOURCE AND NUCLEAR OBSCURATION

Kazushi Iwasawa,[1] Hideyo Kunieda, and Yuzuru Tawara
Department of Astrophysics, Nagoya University, Chikusa-ku, Nagoya, 464-01, Japan

Hisamitsu Awaki and Katsuji Koyama
Department of Physics, Kyoto University, Sakyou-ku, Kyoto 606-01, Japan

Takashi Murayama and Yoshiaki Taniguchi[1]
Astronomical Institute, Tohoku University, Aoba, Sendai 980-77, Japan

Received 1994 November 29; revised 1995 April 17

ABSTRACT

We report x-ray and optical spectroscopic observations of an *IRAS*-selected Seyfert 2 galaxy IRAS 18325−5926. The first x-ray observation of this object was made using the Ginga LAC. The x-ray source is found to be highly variable on time scales of 10^3–10^4 s, similar to those of Seyfert 1 nuclei. The x-ray spectrum is well described by power-law continuum with a photon-index $\Gamma \simeq 2.2$ modified by photoelectric absorption intrinsic to the source with $N_H \simeq 1.4 \times 10^{22}$ cm^{-2} and a broad ($\sigma \approx 0.6$ keV) iron K line. The absorption corrected x-ray luminosity in the 2–10 keV band is $L_X = 5.4 \times 10^{43} h_{50}^{-2}$ ergs s^{-1}. We obtained new optical spectra in red and blue bands, which show the strong emission lines of typical Seyfert 2s with a heavy reddening ($A_V = 3.5$ mag). A blue asymmetry is obvious in some strong emission lines and we can resolve narrow (FWHM$\simeq$450 km s^{-1}) and slightly blueshifted ($\simeq$160 km s^{-1}) broad (FWHM$\simeq$1200 km s^{-1}) components. The optical classification of Seyfert 2s can be explained in terms of nuclear obscuration which may occur in the form of a "global" covering rather than in the form of a torus inferred from the unified model, since the extinction derived from optical and x-ray data are comparable. This fact suggests that the hypothesis in which the classification between Seyfert 1's and 2's depends on the orientation is not complete, and a global obscuration is likely to dominate the dusty *IRAS* galaxies with Seyfert 2 characteristics. © *1995 American Astronomical Society.*

1. INTRODUCTION

One of the most important achievement of the *IRAS* mission was the discovery of a large number of infrared galaxies. Although starburst activity dominates most of these, active galactic nuclei (AGNs) emitting nonthermal radiation have been also discovered. Comparison between pre-*IRAS* AGNs and *IRAS*-selected AGNs is interesting. A "warm" *IRAS* color, or flat spectral index between 25 and 60 μm, was suggested as an indicator of the presence of AGN in the *IRAS* galaxies (de Grijp *et al.* 1987). Interestingly, type 2 objects dominate *IRAS* AGNs (the fraction is ~70% in the de Grijp sample), whereas type 1 objects occupy a large fraction of the optical/UV-selected AGNs.

IRAS 18325−5926 is one of the *IRAS* discovered type 2 Seyfert galaxies selected by the "warm" *IRAS* color ($\alpha_{25-60} = -0.94$, and $f_{60_{\mu m}} = 3.17$ Jy: de Grijp *et al.* 1985, 1987, 1992). The host galaxy Fairall 49 is identified as the *IRAS* source, and a distance of 119 Mpc was derived from the redshift $z = 0.0198$ (the Hubble constant $H_0 = 50$ km s^{-1} Mpc^{-1} is assumed throughout this paper). Carter (1984) claimed that this galaxy should be classified as a Seyfert 1.8 since weak broad wing emission exists at the base of the Hβ emission-line profile and low ionization lines such as [O I]λ6300 and [N I]λ5199 are relatively strong. In the recent optical/near-infrared polarization survey of AGNs (Brindle *et al.* 1990a), IRAS 18325−5926 is found to be the highest polarized object ($P = 5.71\% \pm 0.23\%$ at the V band) among narrowline objects in the sample.

The x-ray source H1829−591 (Piccinotti *et al.* 1982) detected by HEAO 1 A-2 is identified with this galaxy (Ward *et al.* 1988). Since the EXOSAT observation resulted in non-detection in the LE but in detection in the ME, Ward *et al.* (1988) suggested that strong low-energy x-ray absorption might occur due to heavy obscuration in the nucleus. The sensitivity of the Ginga LAC (Large Area proportional Counters; Turner *et al.* 1989) allows us to make a precise x-ray measurements of this galaxy. Together with our new optical spectroscopic observation, we discuss the nature of this *IRAS*-selected Seyfert 2 galaxy.

2. X-RAY DATA

2.1 Observations and Data Reduction

IRAS 18325−5926 was observed by the Ginga LAC on May 17 1989. The LAC experiment is comprised of eight identical proportional counters with a total effective area of

[1]Visiting astronomer, Cerro Tololo InterAmerican Observatory, National Optical Astronomy Observatories, operated by the Association of Universities for Research in Astronomy, Inc., under contract with the National Science Foundation.

 0004-6256/95/110(2)/551/8/$0.90

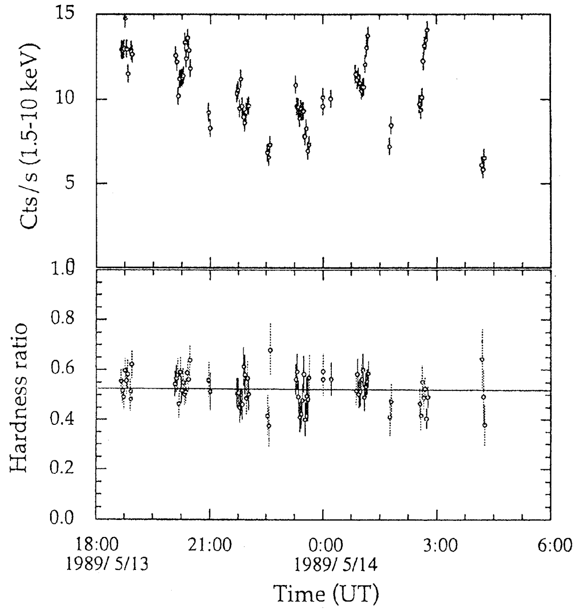

FIG. 1. Light curves observed in the TOP layer in the energy range 2–10 keV, and ratios of the count rate in 4–10 and 2–4 keV bands. Whereas the total x-ray flux is highly variable, the hardness ratio plot (lower panel) indicates the spectral slope is almost constant.

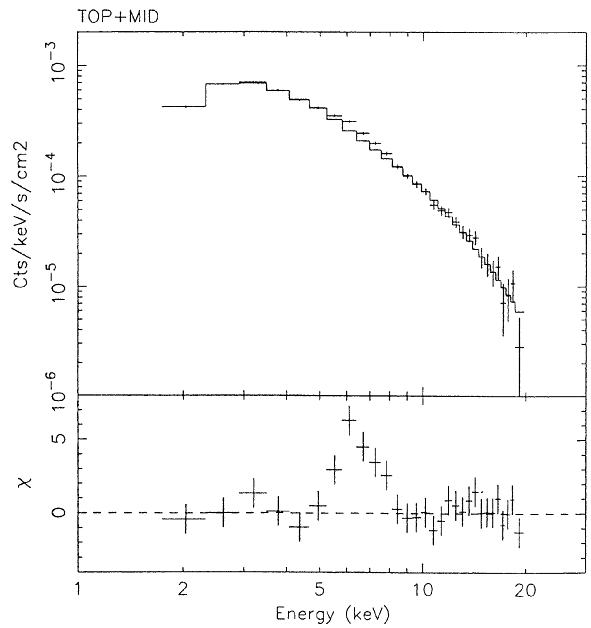

FIG. 2. The 2–20 keV x-ray spectrum of IRAS 18325−5926 observed by TOP+MID layers of the Ginga LAC (upper panel). The solid line represents the best-fitting power-law continuum (see Table 1). A broad iron K line is obvious around 6.24 keV (in the observed frame) in the residual plot (lower panel).

4000 cm^2. The collimated field of view is 1°×2° FWHM. Each counter has two detection layers, the TOP layer sensitive to x-rays in 1–20 keV, and MID layer sensitive to x-rays above 6 keV. The data processing mode MPC-1, which provides pulse-height spectra in the range of 0–37 keV, is divided into 48 energy channels in both TOP and MID layer. The spectral resolution of the LAC at the Fe K band (~6 keV) is $\Delta E/E \approx 20\%$. Observation using the low bit rate allowed 16 s time resolution.

Five linear scans over the position of IRAS 18325−5926 were performed on May 12 1989. The x-ray source was detected at the position of the galaxy. Two other sources were also detected along the scan path at both sides of the *IRAS* galaxy. However, since the two serendipitous sources are located well outside of the LAC field of view in the pointing observation, we safely ruled out any contamination in the observed spectrum. The x-ray intensities and coarse spectra of the two sources are available in the *Ginga Faint Source Catalog* (Awaki *et al.* 1995).

In order to obtain a reliable x-ray spectrum, we discarded the data during periods of high background. The remaining data with integrated exposure time of 8.7×10^3 s in the pointing mode were used to construct the x-ray spectrum of IRAS 18325−5926. We subtracted the non-x-ray background and the cosmic diffuse x-ray background (CXB) separately, using the method described in Awaki *et al.* (1991a). The local CXB was obtained from the observation of a nearby blank field. We should note that during the background observation, an active galaxy ESO 103−G35 which is an x-ray source (e.g., Warwick *et al.* 1993) was present at the edge of the LAC field of view where the transmission efficiency of the collimator is 4%. We took this contamination into account when estimating the normalization of the CXB. The source count rate in the TOP layer of the integrated spectrum, after subtracting the background, was 11.5±0.08 counts s^{-1} in the 2–20 keV band.

As shown in Fig. 1, obvious flux changes on various time scales of ranging from 10^3 to 10^4 s can be seen. The shortest doubling time was ~1500 s in this observation. This indicates the presence of a compact central source similar to Seyfert 1 nuclei. Such rapid variability has been observed in

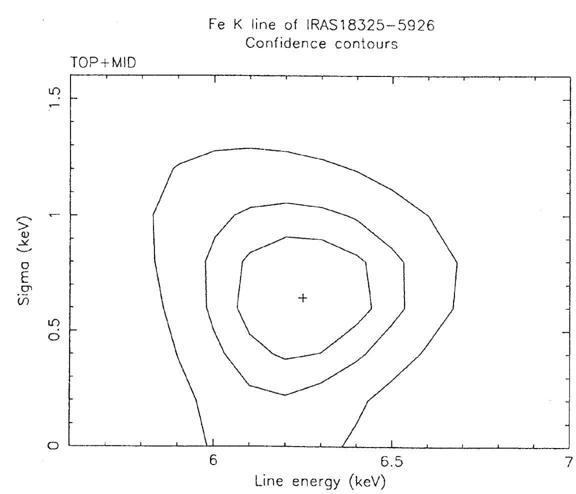

FIG. 3. Confidence contours of the line energy and the linewidth (σ of Gaussian after removing the instrumental response) for the iron K line feature. Contour levels are at 68%, 90%, and 99%. The line profile is significantly broad with above 90% confidence.

TABLE 1. Spectral fits to x-ray data.

(1) Model	(2) Γ	(3) N_H ($\times 10^{22}$cm^{-2})	(4) E_{edge} (keV)	(5) τ	(6) E_{line} (keV)	(7) σ (keV)	(8) EW (eV)	(9) χ^2/dof
NL	2.24 ± 0.05	1.43 ± 0.2	—	—	6.28 ± 0.20	0.05	227 ± 66	22.93/25
BL	2.25 ± 0.05	1.40 ± 0.2	—	—	6.37 ± 0.20	0.63 ± 0.31	430^{+150}_{-100}	16.71/24
NL	2.16 ± 0.05	1.25 ± 0.2	$8.8^{+1.0}_{-0.7}$	0.18 ± 0.14	6.28 ± 0.20	0.05	190 ± 70	17.83/23
BL	2.21 ± 0.05	1.33 ± 0.2	8.8 ± 1.0	$0.09^{+0.18}_{-0.09}$	6.35 ± 0.20	0.55 ± 0.3	390 ± 150	16.00/22

Cols.— (1): Fitting models. In the model of NL, the line width of Fe K is assumed to be narrow (σ = 0.05 keV) whilst it is left to be free in the BL model. (2): Photon-index of power-law. (3): Hydrogen column density corresponding to the low energy cut-off in unit of 10^{22}cm^{-2}. (4): Threshold energy of the iron K-shell absorption edge in the rest frame. (5): Optical depth of the edge absorption at the threshold energy. (6): Peak energy of Gaussian for the iron K emission line in the rest frame. (7): Line width (σ of Gaussian). (8): Equivalent width of the line. (9): Chi-squared value and the degrees of freedom.

other Seyfert 1 nuclei including MCG-6−30−15 (Nandra *et al.* 1990) and IRAS 13224−3809 (Boller *et al.* 1993).

2.2 *Spectral Fitting*

We fit the integrated spectrum from the sum of TOP and MID layers with a power-law model modified by the photoelectric absorption occurring along the line of sight (Fig. 2). The absorption cross section is taken from Morrison & McCammon (1983). The fit was unacceptable due to the presence of an emission-line feature around 6 keV. We used a Gaussian to describe the line feature identified with iron $K\alpha$. Fixing the linewidth to be narrow (i.e., σ of the Gaussian is assumed to be 0.05 keV), the line energy of 6.28±0.2 keV (redshift corrected) and the EW=227±66 eV are obtained. If the linewidth is allowed to be free, we obtain the following characteristics of the iron emission; line energy 6.37±0.2 keV, linewidth σ=0.6±0.3 keV (see Fig. 3), and the equivalent width EW=430^{+150}_{-100} eV. The quality of fit is significantly improved from the narrowline case ($\Delta\chi^2$=6.2, F=8.9). In both cases, the continuum is well described by an absorbed power law with photon index Γ=2.24±0.06 and the absorption column density N_H=(1.43±0.2)×10^{22} cm^{-2}. The N_H value exceeds the corresponding galactic extinction [E($B-V$)=0.09] and implies that the absorption of soft x rays originates in cold material intrinsic to the galaxy. An additional Fe K absorption edge also improves the fit only for the case of narrow Fe $K\alpha$ line. The threshold energy E_{edge}=$8.8^{+1.0}_{-0.7}$ keV clearly rules out cold iron and He-like iron is preferred (Fe XX–Fe XVI are inferred within the 90% confidence range). At the threshold energy, an optical depth τ=0.18±0.14 is obtained. For the broadline case, the iron edge is not significant and the optical depth is constrained to be less than 0.27 at E_{edge}=8.8 keV.

Although the simple absorbed power law can describe 2–20 keV continuum well *without* a "high-energy hump" which is seen in many Seyfert 1 nuclei (Nandra & Pounds 1994), we also tried a power-law model modified by Compton reflection in cold, optically thick material (Lightman & White 1988). The quality of fit (χ^2=15.5 at 23 degrees of freedom) is comparable to that of the simple power-law model. Even though a slightly steeper intrinsic slope $\Gamma\simeq$2.4 is obtained, the lack of improvement of the fit means that the reflection strength (or geometry of the reflection material) cannot be constrained. The results of above spectral fittings are summarized in Table 1. Any spectral change accompanying the flux variation is not obvious within the uncertainties. The averaged x-ray flux observed by Ginga is 3.5×10^{-11} ergs cm^{-2} s^{-1} in the 2–20 keV band. The absorption corrected x-ray luminosity in the 2–10 keV band was L_X=5.4×10^{43} ergs s^{-1}, well within the range for Seyfert 1s.

3. OPTICAL DATA

3.1 *Observations and Data Reduction*

The spectroscopic observations of IRAS 18325−5926 were obtained using the 1.5 m telescope of Cerro Tololo InterAmerican Observatory, National Optical Astronomy Observatories, in August and September 1992. The 1.5 m CCD spectrometer consists of a GEC CCD detector system mounted on a f/7.5 Cassegrain spectrograph. Two gratings (Nos. 16 and 35) were used to obtain blue (4000–5500 Å) and red (6000–7000 Å) spectra. Spectral resolutions with a 3 arcsec slit were 3.7 and 3.2 Å for the blue and the red spectral regions, respectively. We obtained two blue and two red spectra with total exposures of 3600 and 2100 s, respectively. The data were reduced with using IRAF.[1] The reduction was made using the standard procedure of bias subtraction and flatfielding with the data of the dome flats. Flux calibration was obtained using a CTIO standard star (Hamuy *et al.* 1992). The observations were made under photometric conditions. The two independent spectra were stacked into one spectrum for the blue and the red regions in order to improve signal-to-noise ratio. The central 3 arcsec spectrum was extracted for each spectral region. The final blue and red spec-

[1]IRAF is the imaging analysis software package developed by NOAO.

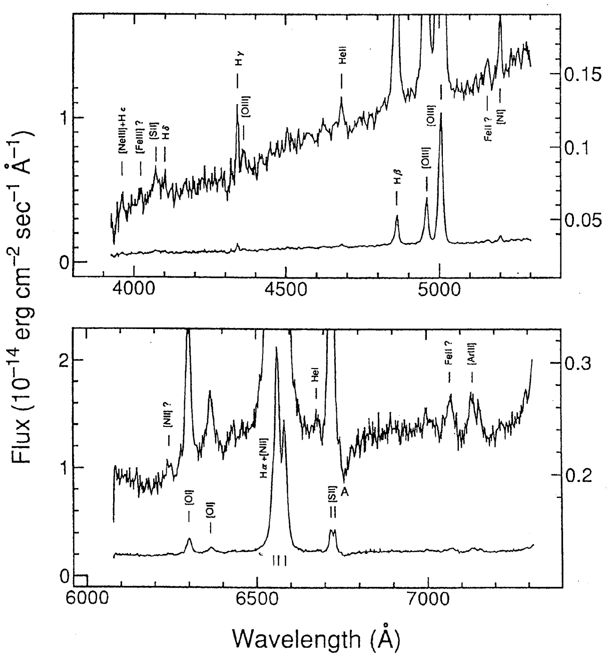

FIG. 4. The blue and the red spectra of IRAS 18325−5926.

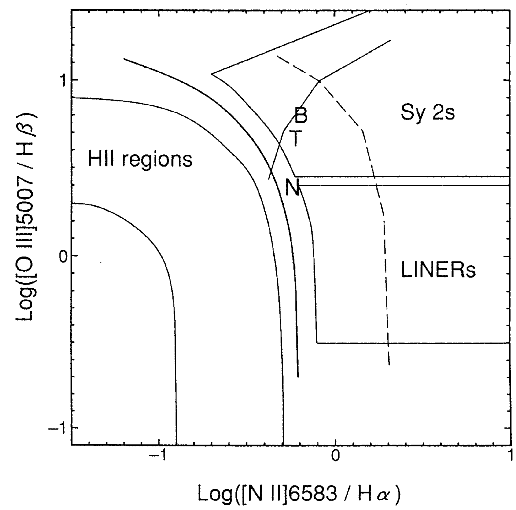

FIG. 5. A diagram of emission-like ratios between [N II]λ6584/Hα and [O III]λ5007/Hβ. The symbols N, B, and T means the data for the narrow, the broad, and the total flux ratios.

tra are shown in Fig. 4. The faint emission features are also shown. The identified emission lines are summarized in Table 2.

3.2 Emission-Line Spectra

The overall optical spectrum (Fig. 4) shows that IRAS 18325−5926 is a typical Seyfert 2 galaxy. In order to identify the excitation condition of the ionized gas in Fig. 5, we give a diagram of emission line ratios between [N II]λ6584/Hα and [O III]λ5007/Hβ (cf. Baldwin *et al.* 1981; Veilleux & Osterbrock 1987). The data point deduced from the total flux is located in the domain of the Seyfert 2 galaxies, although the observed [O III]λ5007/Hβ ratio, 5.44, is close to the lower extreme of Seyfert 2 galaxies (10.0±4.5: from a compilation by Whittle 1992). The [O III]λ5007 emission-line luminosity [log $L_{[\mathrm{O\,III}]}$λ5007(ergs s^{-1})=41.40] is very close to the mean value of Whittle's Seyfert sample [log $L_{[\mathrm{O\,III}]}$λ5007(ergs s^{-1})=41.44]. In the diagram of the hard x ray and [O III]λ5007 luminosities [Fig. 3(c) in Mulchaey *et al.* 1994], IRAS 18325−5926 is found at the middle of the correlation. In this regard, IRAS 18325−5926 is therefore very typical of other Seyfert galaxies in both its x-ray and [O III]λ5007 line strengthens.

The strong emission lines such as Hβ and [O III] lines show evidence for the blueward line asymmetry. This feature is frequently observed in many Seyfert 2 galaxies (cf. Heckman *et al.* 1981; Whittle 1985, 1992; Dahari & De Robertis 1988). The CCD readout produces a weak wing-like feature (see Fig. 6). Since, this effect seems to be small (less than a few percent of the flux), the observed blueward asymmetry of the emission lines are considered to be real. In Fig. 7, we show the results of a two-component Gaussian fitting of the Hβ, [O III]λ4959, and [O III]λ5007 emission lines. These lines are well decomposed into narrow (FWHM≃450 km s^{-1}) and broad (FWHM≃1200 km s^{-1}) components. These line-velocity widths are corrected for the instrumental resolution. The linewidth of the narrow component is comparable to the median value of Seyfert 2 galaxies (510 km s^{-1}: Feldman *et al.* 1982). The broad component is blueshifted by 160 km s^{-1} with respect to the narrow one. The redshifts derived from the narrow components are consistent with those derived with low-ionization lines such as [O I]λ6300, giving z=0.01982±0.00006 after the heliocentric correction. We note that the redshift of 0.0196 derived in previous work (Carter 1984; de Grijp *et al.* 1985) may be affected by the blueshifted broad components.

Although the Hα and [N II]λλ 6548,6584 emission lines show no obvious line asymmetry, we are able to decompose them in the same way. The results are shown in Fig. 8 and Table 2. It is remarkable that a very broad component (FWHM≃3400 km s^{-1}) of Hα emission is necessary to fit the spectra. This component amounts to about 20% of the total Hα emission. Note that as modeling using a Gaussian does not always fit the line asymmetry well, poor modeling could result in an artificial very broad component. If it is real, this component may come from the broadline region observed in Seyfert 1 galaxies. There is no hint of such very broadline component in the Hβ emission, suggesting that IRAS 18325−5926 belongs to the Seyfert 1.9 galaxy class (cf. Osterbrock 1989) rather than the Seyfert 1.8 class (Carter 1984) or Seyfert 2 class (de Grijp *et al.* 1985). Alternatively, IRAS 18325−5926 could be a variable in terms of brightness of the broadline region.

We are able to estimate the reddening of the emitting region by comparing the observed Balmer decrement (the Hα/Hβ ratio) with the theoretical one (3.1: case B with $T_e=10^4$ K and $N_e=10^4$ cm^{-3}: Osterbrock 1989). We find A_V=2.7 and 3.4 mag for the narrow and the broad components. For the total Hα/Hβ ratio, we obtain A_V=3.5 mag.

TABLE 2. Optical emission-line properties.

Identification		λ_{obs}	λ_{rest}	FWHM(km/s)	F/F(Hβ N+B)	I/I(Hβ N+B)
[Ne III], Hϵ		4039.3	3960.5	784	0.075	0.188
[Fe III]?		4102.4	4022.4	1128	0.066	0.155
[S II], [Fe V]?		4153.2	4072.2	1899	0.179	0.398
Hδ		4182.5	4100.9	736	0.056	0.121
Hγ		4426.8	4340.4	527	0.160	0.270
[O III]		4447.7	4360.9	883	0.092	0.152
He II		4776.4	4683.2	1157	0.148	0.177
Hβ	B	4954.7	4858.0	1225	0.576	0.578
	N	4957.8	4861.1	462	0.424	0.424
[O III]	B	5054.2	4955.6	1200	1.44	1.31
	N	5057.3	4958.6	453	0.406	0.368
[O III]	B	5103.2	5003.6	1189	4.24	3.67
	N	5106.2	5006.6	448	1.20	1.04
Fe II, [Fe VII]?		5260.6	5158.0	924	0.135	0.104
[N I]		5303.6	5200.1	581	0.176	0.131
[N II]?, [Al II]?		6367.2	6243.0	1013	0.125	0.045
[O I]		6425.9	6300.5	815	0.921	0.323
[O I]		6490.6	6364.0	807	0.307	0.103
[N II]	B	6675.3	6545.1	1160	1.28	0.380
	N	6678.9	6548.6	452	0.939	0.279
Hα	B	6690.3	6559.8	1157	5.76	1.70
	N	6693.9	6563.3	451	4.80	1.41
	VB	6692.9	6562.3	3434	2.49	0.732
[N II]	B	6711.3	6580.4	1154	3.77	1.09
	N	6714.9	6583.9	450	2.77	0.798
He I		6811.6	6678.7	801	0.103	0.028
[S II]		6852.3	6718.6	601	1.10	0.298
[S II]		6863.9	6730.0	288	0.457	0.123
Fe II?, He I?		7209.4	7068.7	1177	0.315	0.072
[Ar III]		7277.4	7135.4	931	0.322	0.071
F(Hβ N+B)		=		2.75×10^{-14}		
c(Hβ)		=		1.52		
A_V		=		3.51		

Note. — The fifth column gives observed line fluxes normalized to total Hβ. The sixth column gives the relative intensities which are dereddened.

This reddening is heavier by a factor of 3 compared with those of Seyfert 2 galaxies (Dahari & De Robertis 1988).

4. DISCUSSION

4.1 X-ray Properties

The x-ray data obtained from our Ginga observation revealed that the central source of IRAS 18325−5926 has a Seyfert 1-like nature in terms of its x-ray luminosity and variability. The absorption corrected 2–10 keV x-ray luminosity, $L_X \approx 5.4\times10^{43}$ ergs s^{-1} is well within the luminosity range of Seyfert 1s. We also confirm that IRAS 18325−5926 follows the $L_X - L_{IR}$ relation found by Ward *et al.* (1988).

The x-ray variability of Seyfert 2 nuclei has not yet been well studied. There are only a few objects known to be variable. Mrk 3 was found to be variable on a time scale of at least a few years (Iwasawa *et al.* 1994). Possible short term variability (~several hours) in heavily obscured nuclei was observed only from NGC 4945 (Iwasawa *et al.* 1993; Mushotzky *et al.* 1993). IRAS 18325−5926 is the first example of such clear x-ray variation on time scales as short as 10^3–10^4 s which is typically seen in Seyfert 1s.

We find evidence for a broad iron K line with $\sigma \simeq 0.6$ keV (corresponding to FWHM$\simeq 7\times10^4$ km s^{-1}) which is significantly broader than those from the optical BLR. Sometimes poor modeling of the continuum emission may produce a spurious broadline. The narrowline plus additional absorption edge model indeed gives a fairly good fit. However, the broad iron K emission has been verified in a recent ASCA observation (Iwasawa *et al.* 1995). The broad iron line may originate at the innermost region of an accretion disk, within a few tens of the gravitational radius. The profile of a line arising in the relativistic disk may be modified depending on the disk orientation or blackhole metric (e.g., Fabian *et al.* 1989; Chen & Halpern 1989). The medium-resolution x-ray spectrum provided by ASCA is consistent with such a characteristic profile. Since the Gaussian centroid energy (6.37 $\pm$0.2 keV) is consistent with cold Fe, the line may be broadened by Doppler motion which is expected from highly inclined disk. An edge-on disk also produces little reflection (George & Fabaian 1991) consistent with our observation, but the large EW is hard to explain. An alternative solution is the case of a highly ionized disk. If a single broad Gaussian is fit to a relativistic line from a face-on disk where the effect of gravitational redshift is pronounced, then the Gaussian centroid is shifted towards lower energies by >0.2 keV (see Mushotzky *et al.* 1995). If this is the case of IRAS 18325 −5926, the Gaussian center energy may suggest a larger intrinsic line energy indicative of higher ionization. Reflection from highly ionized matter can also account for the lack of the high-energy hump in this object (Ross & Fabian 1993; Matt *et al.* 1993).

There is some disagreement between the x-ray spectra of IRAS 18325−5926 and classical Seyfert 1s. The power-law slope $\Gamma \simeq 2.24\pm0.06$ is steeper than the "canonical" one ($\Gamma \simeq 1.7$) measured using EXOSAT (Turner & Pounds 1989) and HEAO-1 (Mushotzky 1984) from Seyfert 1s. Recently, Nandra & Pounds (1994) reported that the intrinsic slope of Seyfert 1 nuclei in the 2–20 keV range should be $\Gamma = 1.95 \pm 0.05$ after taking into account the effect of the Compton reflection in cold material (e.g., Lightman & White 1988) which can flatten the power-law continuum above ~10 keV. Our results for both the simple power-law and the reflection-modified power-law models unambiguously indicate that IRAS 18325−5926 has a steeper intrinsic continuum. A highly ionized iron absorption edge is marginally detected, when the line is narrow. The threshold energy $E_{edge} \simeq 8.8$ keV corresponding He-like iron is higher than the mean value of Seyfert 1s (7.92±0.12 keV: Nandra & Pounds 1994). There are two possible origins of the ionized absorber. One is the intervening partially ionized gas screen which lying in the line of sight which has been found in some Seyfert 1 galaxies (e.g., Nandra & Pounds 1992; Fabian *et al.* 1994). This should be located closer to the central source than the cold soft x-ray absorber. The other is ionized reflections material (for example, the accretion disk) which is illuminated by the central source. A sum of the direct and reflection components results in an apparently smeared shallow edge.

4.2 Nuclear Obscuration

We confirmed that IRAS 18325−5926 has a typical Seyfert 2 type optical emission-line spectrum as previously suggested by de Grijp *et al.* (1985) and Carter (1984). However, the x-ray data show the presence of a central source having a Seyfert 1-like nature. Using the unified model, we can describe the optical Seyfert 2 spectrum by nuclear obscuration. However the toroidal geometry of the absorber generally considered may not be appropriate. Here we instead propose a "global" obscuration of the nucleus of IRAS 18325−5926, as illustrated in Fig. 9.

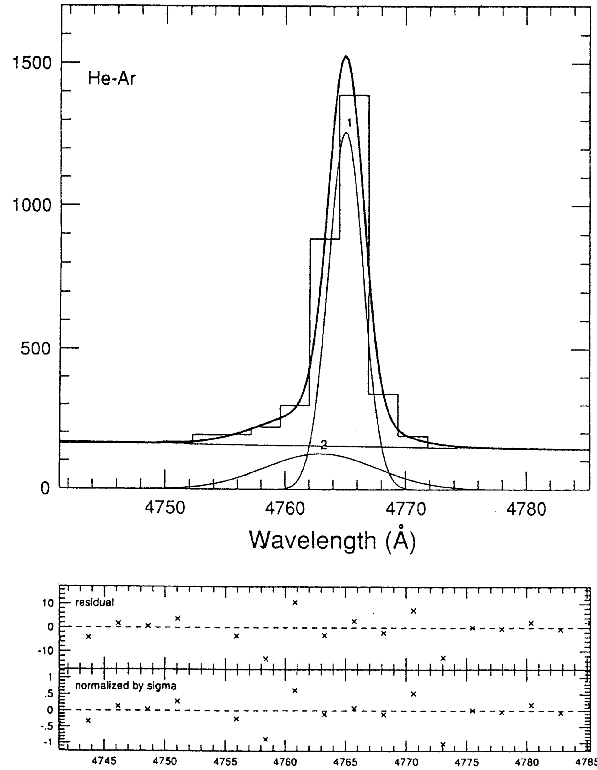

FIG. 6. An instrumental profile of He–Ar line. The effect of the CCD read-out is shown in the weak blue excess emission.

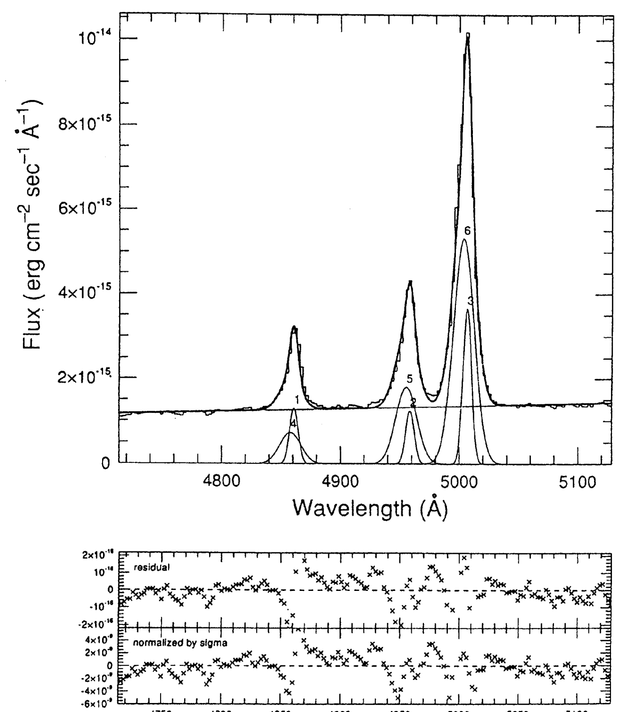

FIG. 7. The result of the Gaussian fit for the Hβ, [O III]λ4959, and [O III]λ5007 emission lines.

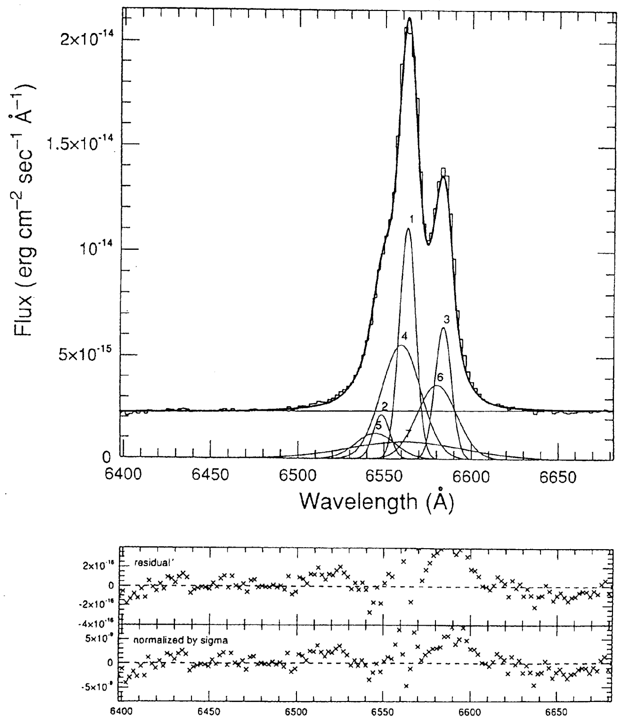

FIG. 8. The result of the Gaussian fit for the Hα, [N II]λ6548, and [N II]λ6584 emission lines. The very broad component of the Hα emission is also shown.

The obscuring torus picture of a Seyfert 2 nucleus has very thick matter in the line of sight. The *BLR* and the central source are hidden, but a small fraction of their radiation is scattered towards us in the uncovered regions close to the symmetrical axis of and above the torus (e.g., Antonucci 1993). The obscuring torus in the line of sight is observed as a cold x-ray absorber of extremely large column density larger than $N_H \sim 10^{23}$ cm^{-2} (Awaki *et al.* 1991b; Koyama *et al.* 1992; Hanson *et al.* 1990; Warwick *et al.* 1993; Mulchaey *et al.* 1994) and up to $10^{24.7}$ cm^{-2} (Iwasawa *et al.* 1993) in classical Seyfert 2 galaxies. On the other hand, in a number of Seyfert 2 galaxies, the obscuration in *NLR* inferred from optical observations is much smaller than the x-ray absorption. In fact, the typical reddening in the *NLR* of Seyfert 2 galaxies is $N_H \simeq 2\times10^{21}$ cm^{-2} (corresponding to $A_V = 1.1$ mag with the standard gas-to-dust ratio: Dahari & De Robertis 1988). The polarized broadline emission (e.g., Antonucci & Miller 1985; Miller & Goodrich 1990) and unabsorbed soft x-ray component (e.g., Koyama *et al.* 1989; Iwasawa *et al.* 1993; Mulchaey *et al.* 1993; Turner *et al.* 1993; Iwasawa *et al.* 1994) found in some Seyfert 2 galaxies indicate the presence of a scattering region not covered by the obscuring material in the nuclei, since they are believed to be hidden behind the obscuring torus and seen only in the scattered light. These observational results support the torus model.

In contrast, the Ginga x-ray spectrum of IRAS 18325−5926 shows a smaller $N_H = 1.4\times10^{22}$ cm^{-2} one to two orders of magnitude below that of the classical sample. The reddening appropriate for the given x-ray extinction using the standard dust-to-gas ratio is comparable to the *NLR* reddening deduced from the Balmer decrement in our optical data. We resolved narrow ($\simeq$450 km s^{-1}) and broad ($\simeq$1200 km s^{-1}) components for the strong lines, Hβ, [O III]λ5007, Hα, and [N II]λ6583, and also a very broad component only at the base of Hα ($\simeq$3400 km s^{-1}). The broadline component appears to be more heavily reddened than the narrow component (see Sec. *3.2*).

The detection of the broad Hα wing provide important information about the obscuration nature, relating to the x-ray luminosity. There is a good correlation between unreddened broad Hα and the 2–10 keV x-ray luminosities in Seyfert 1 galaxies (Ward *et al.* 1988), with average ratio $L_X/L_{H\alpha}\simeq 16$. The flux of the very broad component is 6.8×10^{-14} ergs cm^{-2} s^{-1}, and the ratio is ~200 in IRAS 18325−5926. The reddening required to produce the average ratio observed in relatively unreddened Seyfert 1s is A_V=3.5 mag. This provides a completely independent check of the *VBLR* reddening, which is very similar to the reddening of the broad (FWHM$\simeq$1200 km s^{-1}) component derived from its Balmer decrement. This calculation strongly supports the hypothesis that significant reddening should occur in a dust screen in front of both the *NLR* and *BLR*. There is some internal extinction toward the inner nucleus as implied by the difference in reddening between the 450 and the 1200 km s^{-1} components. However, additional extinction would be unlikely for the very broad (~3400 km s^{-1}) emission-line region from the above calculation. On the other hand, the column density of the x-ray absorbing gas ($N_H\simeq1.4\times10^{22}$ cm^{-2}) implies a larger extinction (A_V~7 mag) assuming the standard gas-to-dust ratio. This means that the innermost part of the nucleus including the 3400 km s^{-1} region is dust-free as noted by Ferland (1990), Netzer & Laor (1993), and Laor & Draine (1993) for the *BLR* in general.

Thus we do not necessarily place the very thick torus in the nucleus of IRAS 18325−5926, but rather prefer a global obscuration. The lack of the reflection component in the x-ray spectrum is also consistent with absence of the cold, thick obscuring torus surrounding the x-ray source, since if it existed out of line of sight, the reflection hump should be pronounced due to the absorption in the cold matter (e.g., Awaki *et al.* 1991b; Krolik *et al.* 1994; Nandra & Pounds 1994; Ghisellini *et al.* 1994).

The *NLR* reddening is heavier by a factor of 3 in A_V than the mean for Seyfert 2s' (Dahari & De Robertis 1990); this provides further evidence for a nucleus shrouded by a large amount of dust. The data are then consistent with a *transmitted* and not *scattered* origin of the weak Hα broad wing as well as the x-ray continuum. In this case, the high polarization could originate by dichroic absorption through the dust grains rather than scattering. This scenario would be compatible with the fact that the wavelength-dependent polarization is well fit with the empirical Serkowski's (1973) curve which describes the transmission of light through aligned dust grains (Brindle *et al.* 1990b).

This obscuration geometry may affect the excitation condition of the optical emission-line region. In the torus model, some of the ionizing radiation from the central source freely escapes into the *NLR* and induces high excitation lines similar to those of Seyfert 1s as observed in classical Seyfert 2 galaxies. However, with global obscuration, the ionizing radiation and particularly the soft x rays are attenuated so that the ionization of the *NLR* resulting is lower than in the torus Seyfert 2s. This idea is consistent with the small [O III]λ5007/Hβ ratio, and strong [O I]λ6300 implying lower ionization (Carter 1984).

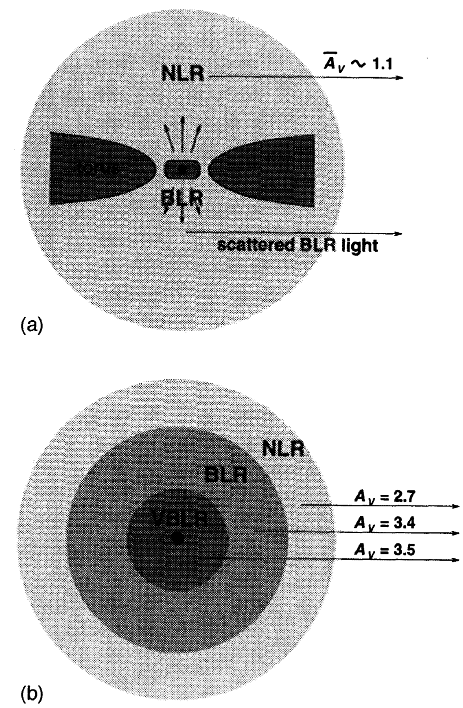

FIG. 9. An illustration of schematic pictures to explain differences in obscuration between (a) the torus model in the unified picture and (b) the global covering model.

Finally, Seyfert 2 galaxies tend to be more molecule rich compared with Seyfert 1s (Heckman *et al.* 1989). Heckman *et al.* (1989) also noted that there is a systematic difference in the far-infrared properties between Seyfert 1 and 2 galaxies. If the dichotomy between Seyfert 1 and 2 nuclei is solely due to the viewing angle, the above observational differences cannot be explained straightforwardly. Recently, Jackson *et al.* (1993) mapped NGC 1068 in HCN emission which traces high-density ($\simeq10^6$ cm^{-3}) gas. They found that the molecular hydrogen column density inferred from the HCN emission amounts to more than 1.3×10^{23} cm^{-2} (corresponding to $A_V\geqslant70$ mag) in the central 600 pc region of NGC 1068. Furthermore, Cameron *et al.* (1994) found that the mid-infrared emission in NGC 1068 is extended over a region of ~70×140 pc. Since the mid-infrared emission comes from dust grains heated by nonthermal continuum radiation from the nucleus, it is unlikely that there is dusty, a few parsec-scale torus in the nucleus of NGC 1068. These lines of evidence strongly suggest that the global covering of the central engine works even in the archetypical Seyfert 2 galaxy NGC 1068.

5. CONCLUSIONS

IRAS 18325−5926 shares the properties of Seyfert 1 nuclei in terms of the x-ray luminosity and its rapid time variability, although the x-ray spectral slope is significantly steeper than that of typical Seyfert 1s. Our optical spectroscopy provides a hint of a very broad line ($\simeq$3400 km s^{-1}) component in the Hα emission, implying the Seyfert 1.9 class rather than typical Seyfert 2. The x-ray variability and the detection of very broad Hα wing imply presence of an obscured Seyfert 1 nucleus. It is remarkable that the column density of the x-ray absorber ($N_H \simeq 1.4\times10^{22}$ cm^{-2}) is much smaller than in the classical Seyfert 2s. A study of the obscuration of the optical emission-line regions suggests a large amount of dust grains in outer part of the nucleus. The observed x-ray continuum and the broad Hα emission is not likely due to *scattering* but *transmission*. The Ginga x-ray spectrum shows no evidence for a torus of cold, thick material. We thus propose a global covering picture rather than the canonical torus model for *IRAS*-selected type 2 objects as well as IRAS 18325−5926.

We would like to thank the science operation team of Ginga and Dr. K. Leighly for critical reading of the manuscript and her comments. We also thank the staff of Cerro Tololo InterAmerican Observatory, in particular, Mark Phillips and Mario Hamuy, for their kind guidance and useful suggestion for the optical spectroscopic observations. KI thanks JSPS for their support of young scientists in the form of fellowships. In the optical observation in CTIO, KI is also supported by the national grant of the international scientific research No. 04041110. Y. Taniguchi thanks Koujun Yamashita for his encouragement.

REFERENCES

Antonucci, R. 1993 ARA&A, 31, 473
Antonucci, R., & Miller, J. 1985, ApJ, 297, 621
Awaki, H., Koyama, K. Kunieda, H., Takano, S., Tawara, Y., & Ohashi, T. 1991a, ApJ, 366, 88
Awaki, H., Koyama, K., Inoue, H., & Halpern, J. P. 1991b, PASJ, 43, 195
Awaki, H., Yamauchi, S., Iwasawa, K., Kamata, Y., Koyama, K., & Tawara, Y. 1995, in preparation
Brindle, C., Hough, H., Bailey, J. A., Axon, D. J., Ward, M. J., Sparks, W. B., & McLean I. S. 1990a, MNRAS, 244, 577
Brindle, C., Hough, H., Bailey, J. A., Axon, D. J., Ward, M. J., Sparks, W. B., & McLean I. S. 1990b, MNRAS, 244, 604
Boller, Th., Trumper, J., Molendi, S., Fink, H., Schaeidt, S., Caulet, A., & Dennefeld, M. 1993, A&A, 279, 53
Baldwin, J. A., Phillips, M. M., & Terlevich, R. 1981, PASP, 93, 5
Cameron, M., Storey, J. W. V., Rotaciuc, V., Genzel, R., Verstraete, L., Drapatz, S., Siebenmorgen, R., & Lee, T. J. 1994, ApJ, 419, 136
Carter, D. 1984, Astron. Express, 1, 61
Chen, K., & Halpern, J. P. 1989, ApJ, 344, 115
Dahari, O., & De Robertis, M. M. 1988, ApJ, 331, 727
de Grijp, M. H. K., Miley, G. K., Lub, J., & de Jong, T. 1985, Nature, 314, 240
de Grijp, M. H. K., Miley, G. K., & Lub, J. 1987, A&AS, 70, 95
de Grijp, M. H. K., Keel, W. C., Miley, G. K., Goudfrooij, P., & Lub, J. 1992, A&AS, 96, 389
Fabian, A. C., *et al.* 1994, PASJ, 46, L59
Fabian, A. C., Rees, M. J., Stella, L., & White, N. E. 1989, MNRAS, 238, 729
Feldman, F. R., Weedman, D. W., Balzano, V. A., & Ramsey, L. W. 1982, ApJ, 256, 427
Ferland, G. J., Korista, K. T., & Peterson, B. M. 1990, ApJ, 363, L21
George, I. M., & Fabian, A. C. 1991, MNRAS, 249, 352
Ghisellini, G., Haardt, F., & Matt, G. 1994, MNRAS, 267, 743
Hamuy, M., Walker, A. R., Suntzeff, N. B., Gigoux, P., Heathcote, S. R., & Phillips, M. M. 1992, PASP, 104, 533
Hanson, C. G., Skinner, G. K., Eyles, C. J., & Willmore, A. P. 1990, MNRAS, 242, 262
Heckman, T. M., Blitz, L., Wilson, A. S., Armus, L., & Miley, G. K. 1989, ApJ, 342, 735
Heckman, T. M., Miley, G. K., van Bruegel, W. J. M., & Butcher, H. R. 1981, ApJ, 247, 403
Iwasawa, K., Koyama, K., Awaki, H., Kunieda, H., Makishima, K., Tsuru, T., Ohashi, T., & Nakai, N. 1993, ApJ, 409, 155
Iwasawa, K., Yaqoob, T., Awaki, H., & Ogasaka, Y. 1994, PASJ, 46, L167
Iwasawa, K., Fabian, A. C., Mushotzky, R. F., Awaki, & H., Kunieda, H. 1995, in preparation
Jackson, J. M., Paglione, T. A. D., Ishizuki, S., & Rieu, N-. Q. 1993, ApJ, 418, L13
Krolik, J. H., Madau, P., & Życki, P. T. 1994, ApJ, 420, L57
Koyama, K., Inoue, H., Takano, S., Tamaka, Y., Ohashi, T., & Matsuoka, M. 1989, PASJ, 41, 731
Koyama. K, Awaki, H., Iwasawa, K., & Ward, M. J. 1992, ApJ, 399, L129
Laor, A., & Draine, B. T. 1993, ApJ, 347, 179
Lightman, A. P., & White, T. R. 1988, ApJ, 335, 57
Matt, G., Fabian, A. C., & Ross, R. R. 1993, MNRAS, 262, 179
Morrison, R., & McCammon, D. 1983, ApJ, 270, 119
Mulchaey, J. S., Koratkar, A., Ward, M. J., Wilson, A. S., Whittle, M., Antonucci, R. R. J., Kinney, A. L., & Hurt, T. 1994, ApJ, 436, 586
Mulchaey, J. S., Colbert, C., Wilson, A. S., Mushotzky, R. F., & Weaver, K. A. 1993, ApJ, 414, 144
Mushotzky, R. F. 1984, Adv. Space Res. 3, 10
Mushotzky, R. F., Fabian, A. C., Iwasawa, K., Kunieda, H., Matsuoka, M., Nandra, K., & Tanaka, Y. 1995, MNRAS, 272, L9
Mushotzky, R. F., Done, C., & Pounds, K. A. 1993, ARAA, 31, 717
Nandra, K., Pounds, K. A., & Stewart, G. C. 1990, MNRAS, 242, 660
Nandra, K., & Pounds, K. A. 1992, Nature, 359, 215
Nandra, K., & Pounds, K. A. 1994, MNRAS, 268, 405
Netzer, H., & Laor, A. 1993, ApJ, 404, L51
Osterbrock, D. E. 1989, Astrophysics of Gaseous Nebulae and Active Galactic Nuclei (Freeman, San Francisco)
Piccinotti, G., Mushotzky, R. F., Boldt, E. A., Holt, S. S., Marshall, F. E., Serlemitsos, P. J., & Shafer, R. A. 1982, ApJ, 253, 485
Ross, R. R., & Fabian, A. C. 1993, MNRAS, 261, 74
Serkowski, K. 1973, in IAU Symposium No. 52, Interstellar Dust and Related Topics, edited by J. M. Greenberg and H. C. van de Hulst (Reidel, Dordrecht), p. 145
Turner, T. J., Urry, C. M., & Mushotzky, R. F. 1993, ApJ, 418, 653
Turner, T. J., & Pounds, K. A. 1989, MNRAS, 240, 833
Turner, M. J. L. *et al.* 1989, PASJ, 41, 345
Veilleux, S., & Osterbrock, D. E. 1987, ApJS, 63, 295
Ward, M. J., Done, C., Fabian, A. C., Tennant, A. F., & Schafer, R. A. 1988, ApJ, 324, 767
Warwick, R. S., Sembey, S., Yaqoob, T., Makishima, K., Ohashi, T., Tashiro, M., & Kohmura, Y. 1993, MNRAS, 265, 412
Whittle, M. 1985, MNRAS, 216, 817
Whittle, M. 1992, ApJS, 79, 49